

Climate Change and the Middle Atmosphere. Part II: The Impact of Volcanic Aerosols

D. RIND, N. K. BALACHANDRAN,* AND R. SUOZZO**

Goddard Space Flight Center, Institute for Space Studies, New York, New York

(Manuscript received 26 December 1990, in final form 26 June 1991)

ABSTRACT

The effects of volcanic aerosols on the middle atmosphere are investigated with the Goddard Institute for Space Studies (GISS) Global Climate/Middle Atmosphere model. Volcanic aerosols with a visible optical depth of 0.15 are put into the lower stratosphere, and their influence is explored for different time scales: instantaneous effect (sea surface temperatures not allowed to adjust); influence for the first few years, with small tropospheric cooling; and long-term effect (50 years) with significant tropospheric cooling.

The aerosols induce a direct stratospheric response, with warming in the tropical lower stratosphere, and cooling at higher latitudes. On the shorter time scales, this radiative effect increases tropospheric static stability at low- to midlatitudes, which reduces the intensity of the Hadley cell and Ferrel cell. There is an associated increase in tropospheric standing wave energy and a decrease in midlatitude west winds, which result in additional wave energy propagation into the stratosphere at lower midlatitudes in both hemispheres. Convergence of this flux in the middle atmosphere increases the residual circulation, producing low-latitude cooling and high-latitude warming near the stratopause. The dynamical changes are on the order of 10%, and are generally similar to occurrences following major volcanic eruptions in the last 30 years.

On the longer time scale, a strong hemispheric asymmetry arises. In the Northern Hemisphere eddy energy decreases, as does the middle-atmosphere residual circulation, and widespread stratospheric cooling results. In the Southern Hemisphere, the large increase in sea ice increases the tropospheric latitudinal temperature gradient, leading to increased eddy energy, an increased middle-atmosphere residual circulation, and some high-latitude stratospheric warming.

The different experiments emphasize that the middle-atmosphere response to climate change depends on both the direct and indirect (i.e., tropospheric) effects. Similarly, the tropospheric changes are not simply the products of the direct climate perturbation; they depend as well on what happens to the stratosphere. Such examples of the coupled systems underline the need to include both the troposphere and middle atmosphere in studying the effects of climate change.

1. Introduction

This paper is a continuation of the study of climate change and the middle atmosphere using the Goddard Institute for Space Studies (GISS) Global Climate Middle Atmosphere Model (GCMAM; described in Rind et al. 1988a,b, henceforth papers A and B). In Part I we investigated the changes due to the doubling of atmospheric CO₂ (Rind et al. 1990, henceforth RSBP). The results contained some surprises, primarily that eddy energy increased in the middle atmosphere despite decreases in the troposphere. This led to an increased transformed Eulerian (or residual) circulation in the doubled CO₂ middle atmosphere, of the

order of 10%–20% of the control run (normal CO₂) values, a change that would have implications for the distributions of ozone and other trace gases. The results apparently depended on the vertical and latitudinal thermal destabilization of the troposphere/middle atmosphere system in response to the increased CO₂, with tropospheric warming maximizing in the tropical upper troposphere, and stratospheric cooling maximizing near the stratopause.

In Part II, we investigate the response of the middle atmosphere to an increase in stratospheric aerosols, nominally associated with increased volcanic activity. The study has several motivations, and so is done in several parts. Volcanic aerosols have been associated with warming of the lower stratosphere in both observations (Newell 1970; Labitzke et al. 1983; Parker and Brownscombe 1983; Quiroz 1983; Fujita 1985; Wandler and Kodama 1986) and models (Hansen et al. 1978; Pollack and Ackerman 1983), associated with increased energy absorption by SO₂ aerosols. Volcanoes have also been implicated in altering the dynamics of the stratosphere. Van Loon and Labitzke (1987) and

* Lamont-Doherty Geological Observatory of Columbia University, Palisades, New York.

** Center for the Study of Global Habitability, Columbia University.

Corresponding author address: Dr. David Rind, Goddard Institute for Space Studies, 2880 Broadway, New York, NY 10025.

Labitzke and van Loon (1989) have noted that the normal association with a warm event in the El Niño–Southern Oscillation (ENSO) in Northern Hemisphere winter is a warm polar vortex and cold tropical stratosphere, with a weak westerly circulation. However, this association has broken down following the eruptions of Mt. Agung in 1963 and El Chichón in 1982, with stratospheric tropical warming, and a cold, stable polar vortex. Exploring the direct effects of volcanic aerosols on the middle atmosphere is thus one of the research goals of these experiments.

In addition, volcanic aerosols can affect the troposphere, primarily through their tendency to cool the climate (e.g., Hansen et al. 1978). As the climate cools, tropospheric dynamics may change, which could conceivably affect the stratosphere. Also, the contrast between the troposphere and stratosphere would be altered, which could have further ramifications. Thus, the other component of this study is to determine how the tropospheric effects of volcanic aerosols may affect the middle atmosphere.

The two parts of this question inherently involve different time scales. To affect the stratosphere, volcanic aerosols need be present for only several months. The large volcanic aerosol injections of the past few decades (Mt. Agung, El Chichón) remained in the atmosphere for several years, and are good examples of this type of forcing. To affect the tropospheric climate fully, the volcanic aerosols would need to be in place for some 50 years, so as to allow the ocean sufficient time to fully cool (Hansen et al. 1985). A possible example of this occurrence, which implies multiple volcanic eruptions, is the Little Ice Age (circa 1600 to 1800), which Porter (1986) has shown coincides with times of increased volcanic activity, as deduced from acidity records in the Greenland ice core. The different time scales thus allow for different ocean responses and different magnitudes of tropospheric response. Nevertheless, even the short-term events may alter tropospheric processes in conjunction with their slight cooling.

In this paper we describe the results of three experiments: one in which volcanic aerosols are put into the stratosphere and the sea surface temperatures are not allowed to change; a second experiment in which the (minimal) sea surface temperature changes that arise in the first three years are utilized; and the third, in which volcanic aerosols are incorporated and maintained in the stratosphere and the sea surface temperatures that occur after ~ 50 years of integration are employed. The first experiment should highlight the effects of the direct stratospheric influence, while the second might add an additional tropospheric response (although in fact there was little difference between the results of experiments one and two). The third experiment includes the much larger tropospheric changes allowed by the longer time scale. The different experiments should further elucidate how the middle atmosphere responds to potential climate perturbations.

2. Experiments

The volcanic aerosols used for this experiment have a visible optical depth (τ) set equal to 0.15, which is held constant in time and space. The volcanic particles are assumed to be made of sulfuric acid (75% H_2SO_4 by weight); thus, they are good scatterers of solar radiation and very good absorbers of thermal radiation (Pollack and Ackerman 1983). A bimodal, lognormal distribution is used to describe their size distribution, with the volume modal radii equal to 0.2 and 0.6 μm , and with the widths equal to 1.6 and 1.2, respectively. Each mode is assumed to contribute equally to τ , and is evenly divided among the levels of insertion. For the smaller particles, τ varies from ~ 0.22 at 0.3 μm to 0.02 at 10 μm , while for the bigger particles it is close to 0.15 at 0.3 μm and 0.05 at 10 μm . The composition and size distribution are based on measured properties of the El Chichón volcanic cloud (e.g., Hofmann and Rosen 1983; Oberbeck et al. 1983); while the details of shortwave versus longwave heating in the lower stratosphere are likely to be sensitive to the size distributions used, the overall heating should be similar for volcanoes with similar visible optical depths and sub-micron particle sizes.

To calculate the scattering characteristics of the aerosols, Mie theory is used in conjunction with the optical constants of sulfuric acid (Palmer and Williams 1975) and the given distribution to evaluate the single-scattering properties of the particles. As these particles are in a liquid phase (e.g., Oberbeck et al. 1983), Mie theory is appropriate.

In order to minimize the amount of computer time involved in the different experiments, we first used the 9-level climate model described in Hansen et al. (1983). The volcanic aerosols were added to this model in its top two layers, whose global average pressures are 102 and 26 mb, respectively. The model, with these aerosols, was run for 55 years. Due to the ocean thermal response time and the feedbacks that appear subsequent to the initial forcing (water vapor, cloud cover, and sea ice changes), the climate alterations induced by the aerosols depend upon the length of time of integration. A full description of these climatological effects is presented in Pollack et al. (1991). For the experiments with the middle-atmosphere model, we make use of the sea surface temperature and other boundary condition changes generated in this 9-layer model, in lieu of integrating the full middle-atmosphere model for the full length of time.

In experiment 1 we utilize the current sea surface temperatures, as in the standard current climate control run (i.e., paper A). The volcanic aerosols are introduced into the different model layers with the distribution shown in Table 1. The model is integrated for three years following a six-month spinup. With unchanging sea surface temperatures the tropospheric cooling is very small; the annual average surface air

TABLE 1. Volcanic aerosol visible optical thickness.

Pressure (mb)	0.2 μm	0.6 μm
149	0.023	0.031
68	0.025	0.034
32	0.012	0.016
15	0.004	0.006

temperature change is -0.08°C . The purpose of this experiment is to minimize as much as possible the influence of volcanic-induced tropospheric changes on the middle atmosphere. As the emphasis is on the direct effect of volcanic aerosols within the stratosphere, this experiment will be referred to as STRAT.

In experiment 2 we investigate the impact of volcanic aerosols that remain in the stratosphere for only several years, as is normally the case. Thus, we use the sea surface temperature changes that arose in the 9-layer model averaged for the first three years; this produced a small tropospheric cooling. The volcanic aerosol vertical distribution is the same as in experiment 1 (e.g., Table 1). The model was then run for three years, after a six-month spinup. The rationale behind this experiment was that it more closely approximates the real world situation for transient volcanic influence. However, as its results differed little from those in STRAT, we will refer to it only occasionally, as the "transient" experiment (TRANS).

In experiment 3 we are interested in the additional effect of allowing the full tropospheric cooling to be included. In this case, we use the average sea surface temperature values from years 46 to 55, with substantial tropospheric cooling (global annual average surface air temperature change of -4.7°C). Again the experiment involves a three-year run, after a six-month spinup. As this experiment includes a strong tropospheric climatological change, it is referred to as CLIM.

Is three years sufficient time to establish a stable stratospheric response, given the model's natural variability (paper B)? To place the changes in perspective, they will be related to standard deviations from the control run; in addition, the similarity of the three-year results in STRAT to those in TRANS implies that the forcing is sufficiently strong to generate a consistent model response.

3. Results

Given the diverse nature of these experiments, we discuss the results of the aerosol impact in three parts: for STRAT and then TRANS, with little tropospheric cooling, and for CLIM with substantial tropospheric cooling.

a. STRAT

Shown in Fig. 1a are the annual average temperature changes between STRAT and the control run. The changes for December–February and June–August are

shown in Fig. 2a,b, and result from processes similar to those described below for the annual average. Following are the major effects that arise:

1) The volcanic aerosols have induced warming in the lower tropical stratosphere, of some three standard deviations of the interannual variability of the control run. (The standard deviations referred to are shown in paper B.) This is a result of both shortwave (Fig. 3a) and longwave (Fig. 3b) absorption effects. The additional shortwave radiative heating (of some 1%–2%) occurs not only in the levels of aerosol input (Table 1) but also above, due to the added reflected light being absorbed by ozone. Reduced longwave cooling would be expected where the atmosphere has cooled, but it also occurs in the tropics at 68 and 149 mb, where the temperature has warmed, due to the longwave absorption properties of the aerosols. At these levels the net longwave radiation change equals or exceeds the warming due to solar radiation absorption. However, the longwave radiation changes are not simply the result of the additional aerosols, as they are also affected by temperature changes induced dynamically.

2) In the tropical middle to upper stratosphere, and continuing into the mesosphere, cooling occurs. This is the result of a general increase in upward velocities associated with an increased residual circulation (Fig. 4a); it is therefore due to a change in dynamical heating (Fig. 4b). These changes are on the order of 5%–15% of the control run values (generally two to four standard deviations for the change in streamfunction, one to two for the dynamical heating).

3) In the polar upper stratosphere and lower mesosphere of both hemispheres, temperatures warm, with a magnitude from one to four times the model's natural variability. This also arises due to changed dynamics, in particular the altered residual circulation (Fig. 4).

4) The polar temperatures in the low- to midstratosphere cool. This is primarily a radiative effect (Fig. 3), from both reduced shortwave heating (as radiation is scattered away) and increased thermal energy radiation. A small dynamical effect also occurs in the Northern Hemisphere, associated with a decrease in the extreme polar portion of the residual circulation (Fig. 4).

5) The tropospheric temperatures cool slightly, especially in the Northern Hemisphere in summer. This is the result of aerosol scattering of incoming sunlight, which increases the planetary albedo by 1.4% (absolute). Its effect on the tropospheric climate is minimized since the sea surface temperatures were not allowed to change.

6) At upper levels in the mesosphere, temperatures warm, also a dynamical effect.

While some of these changes are not large compared to the model's interannual variability, the results noted above also occurred in TRANS, which allowed the sea surface temperatures to adjust for the first three years,

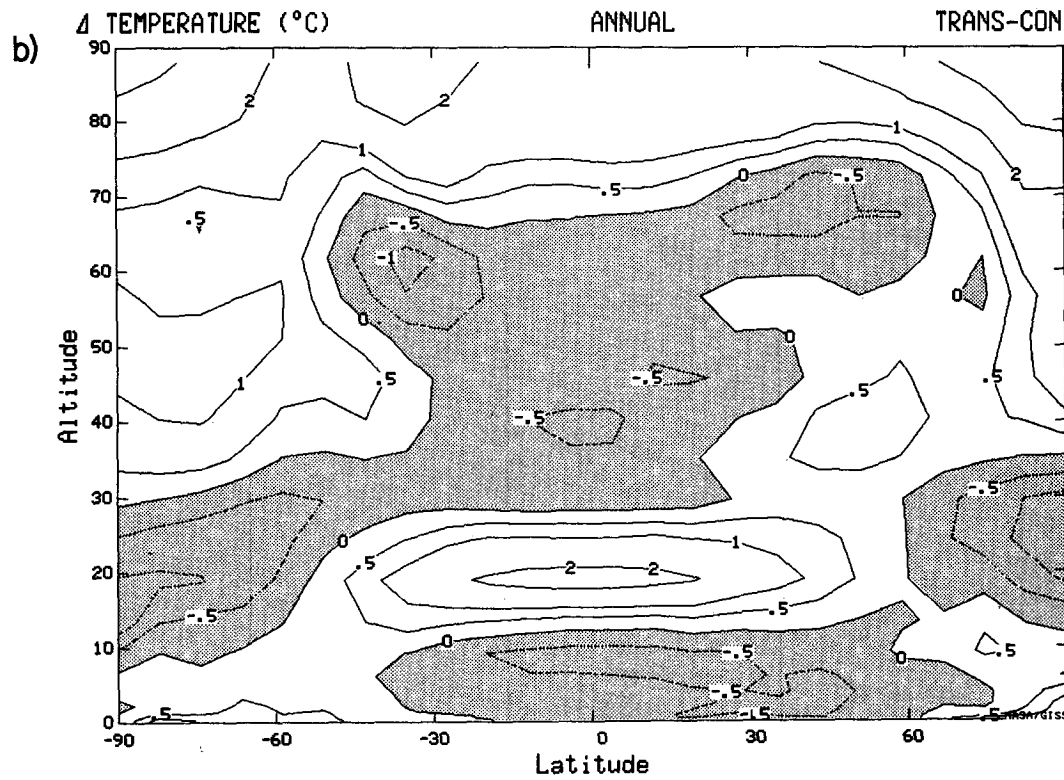
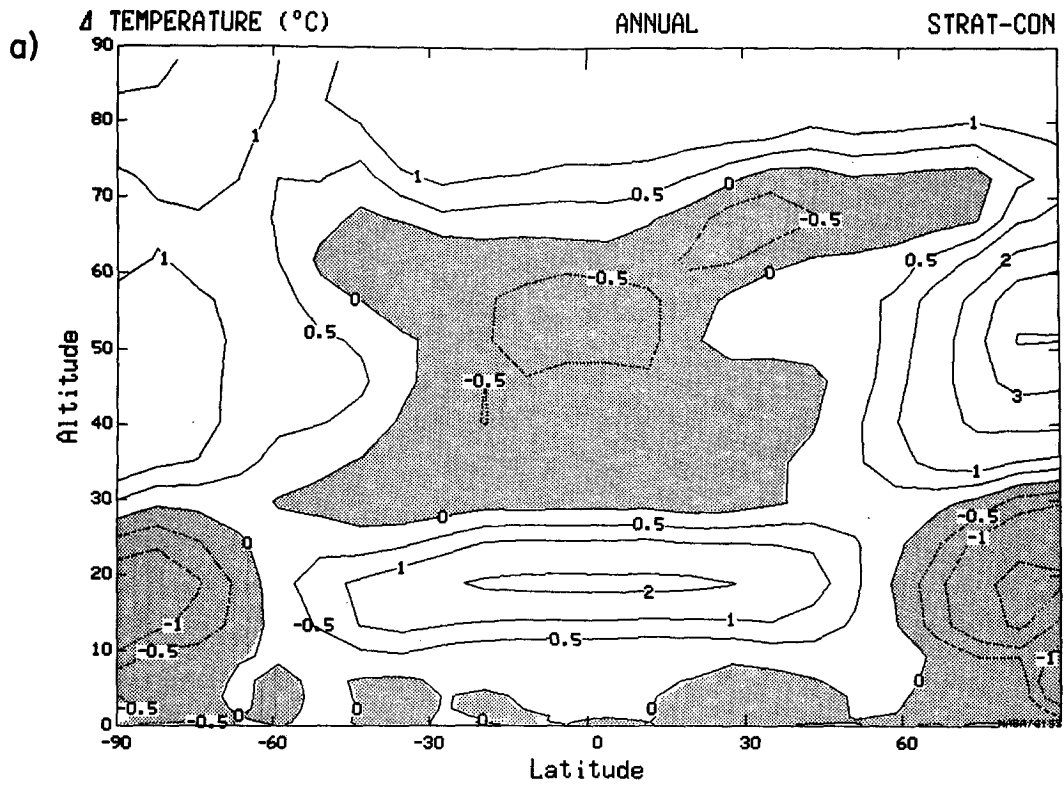


FIG. 1. Annual-average temperature change between (a) STRAT and the current climate control run, and (b) TRANS and the current climate control. Negative values are shaded. Results in this and subsequent figures are averages for three years.

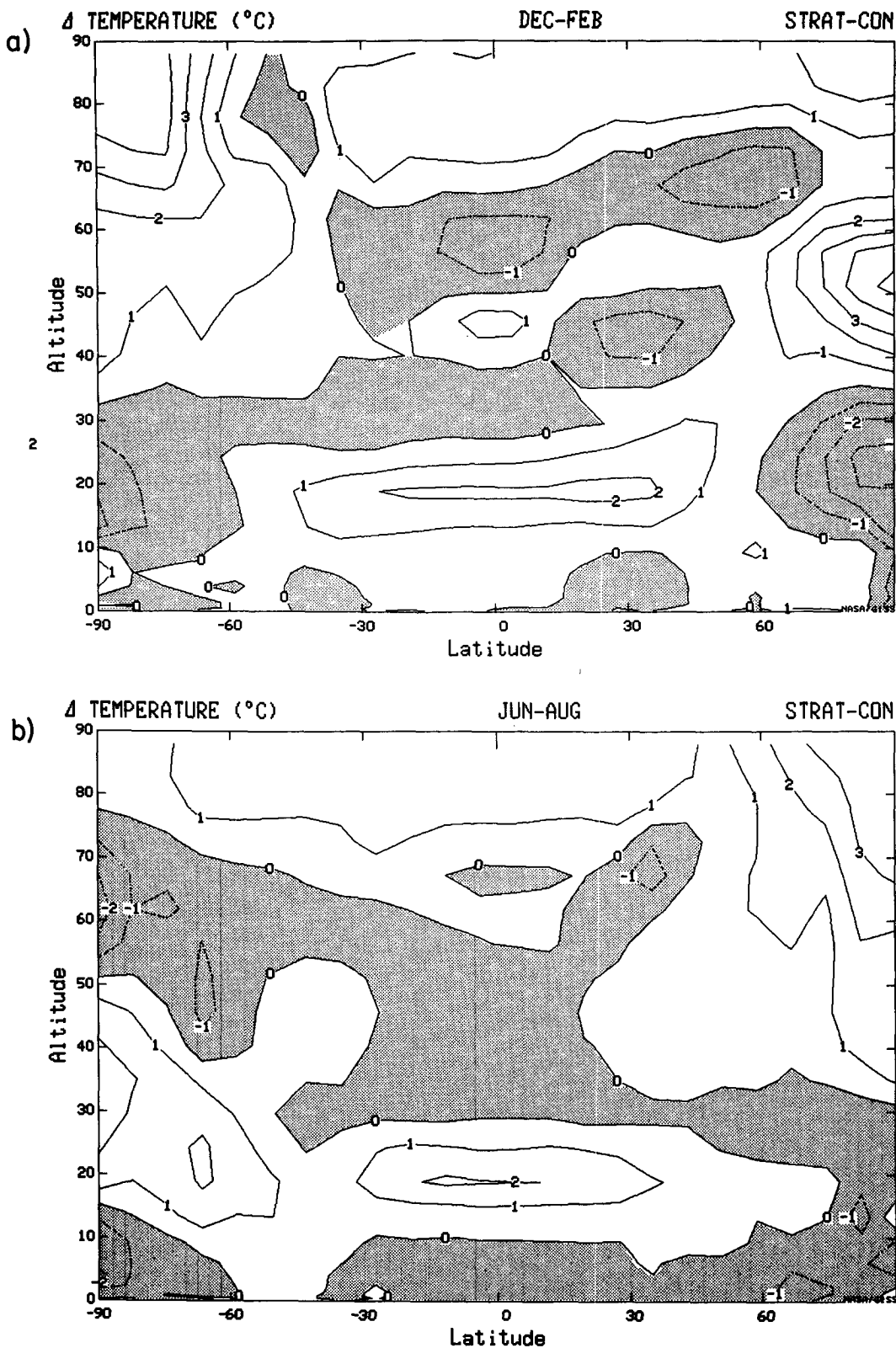


FIG. 2. Temperature changes in STRAT for (a) December-February and (b) June-August.

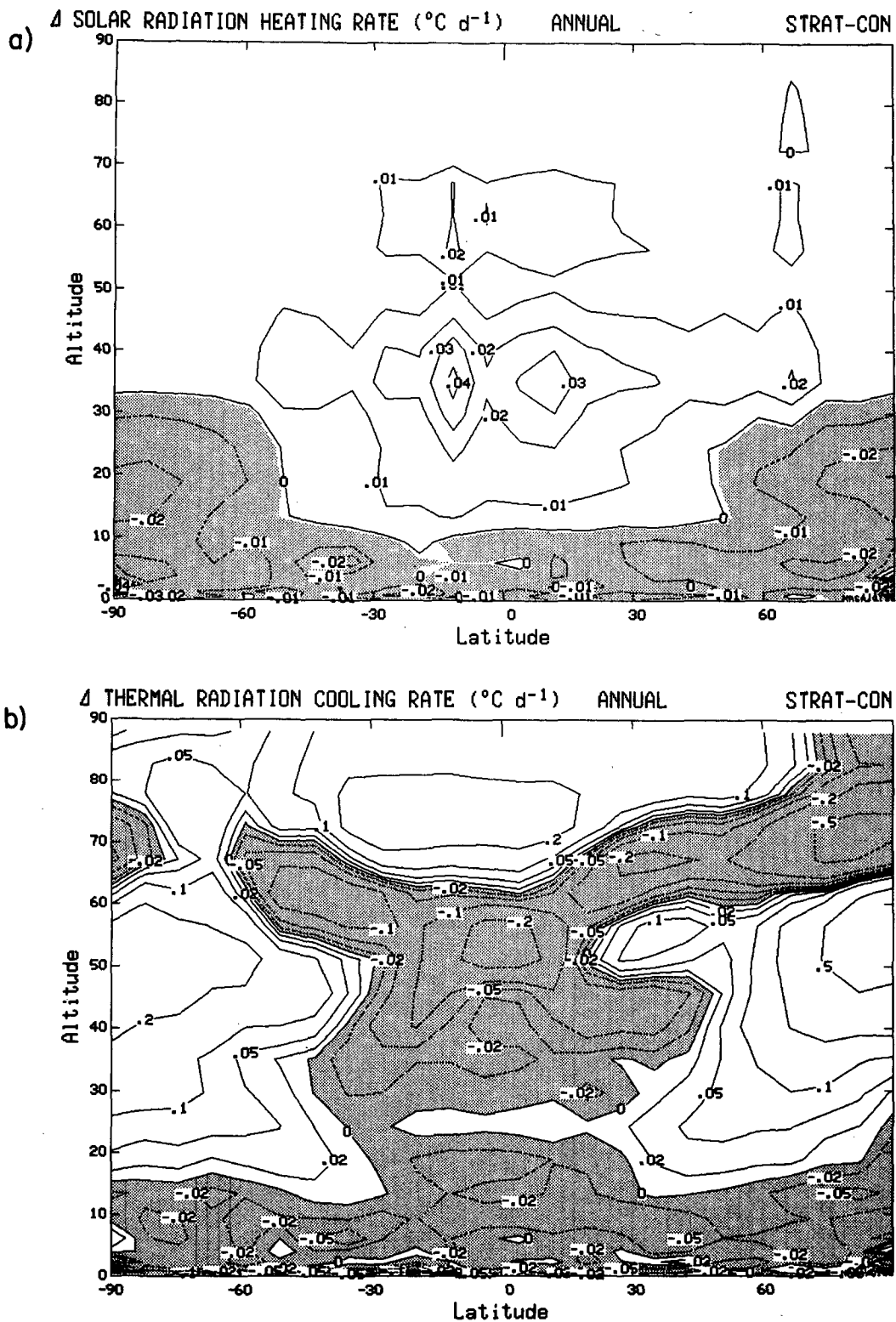


FIG. 3. Change in heating rates between STRAT and the control run for (a) shortwave heating, and (b) longwave cooling. (Note that negative changes in longwave cooling signify heating.)

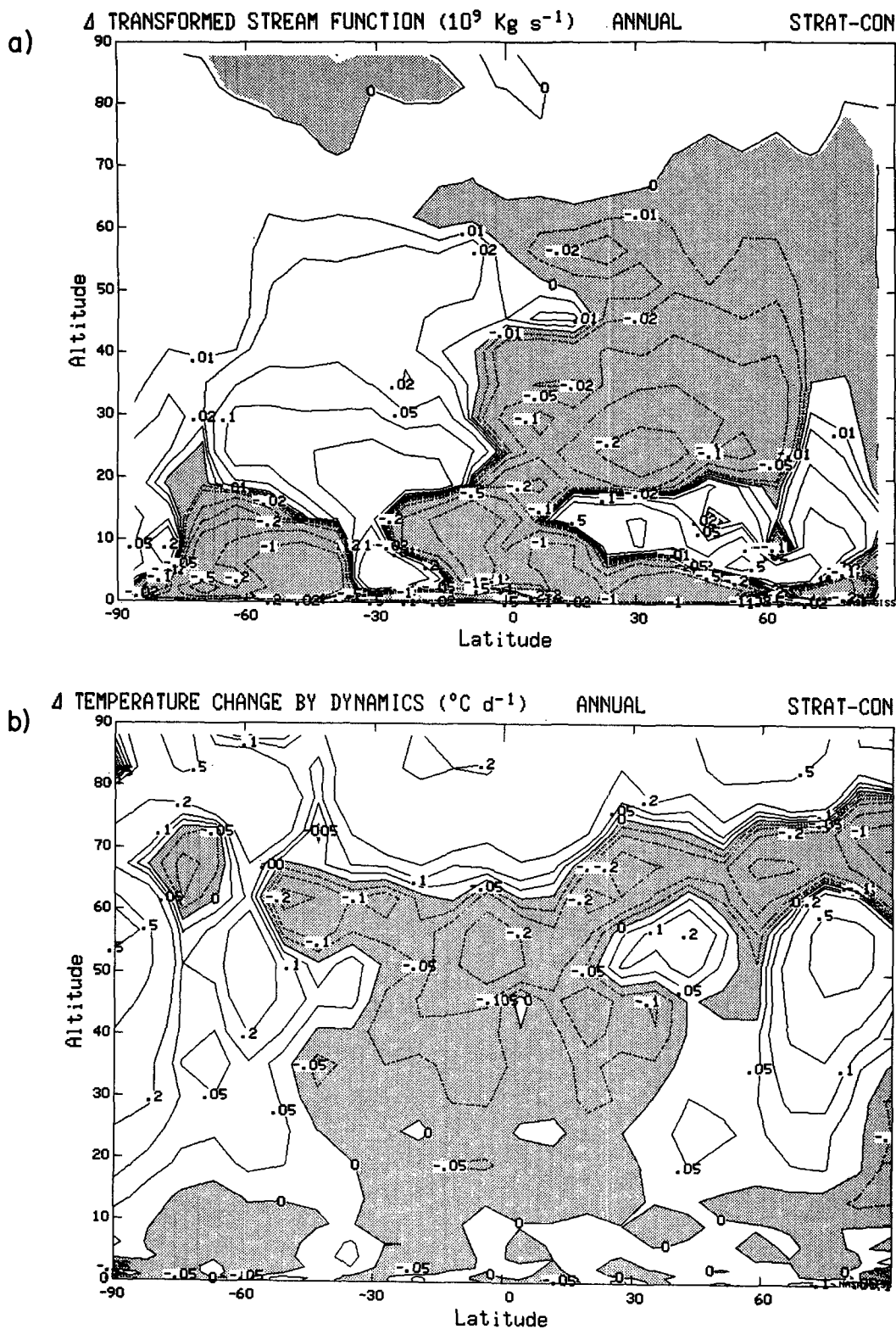


FIG. 4. (a) Annual average changes in STRAT in residual circulation. Negative values mean a greater clockwise circulation in the plane of the paper. (b) Annual average change in heating by atmospheric dynamics between STRAT and the current climate control run.

TABLE 2. Change in eddy kinetic energy (%).

Experiment	984–100 mb									
	EKE		Standing EKE		100–10 mb EKE		10–0.5 mb EKE		0.5–0 mb EKE	
	NH	SH	NH	SH	NH	SH	NH	SH	NH	SH
STRAT	0.6	-1.7	2.3	-2.0	7.4	5.0	5.2	6.8	-0.3	-2.3
TRANS	-1.0	-6.3	1.8	-7.4	7.6	1.4	5.8	2.3	0.4	-2.7
CLIM	-0.5	9.9	3.0	7.4	-3.7	4.6	1.4	8.5	-4.8	-8.9

and thus had slightly greater tropospheric cooling (Fig. 1b). In fact, most of the explanations for the changes turn out to be similar in experiments 1 and 2.

As shown in Fig. 4, in addition to the direct radiative effect generated by the aerosols in the middle atmosphere, there is also a dynamical change influencing the temperature field. The increased transformed streamfunction spiraling away from the equator looks as if it might be associated with the heating of the lower stratosphere, but the magnitude is too great for it to be due to that influence alone: If all the excess heating went into generating vertical motion, the resultant velocity in the lower equatorial stratosphere would be only 20% of the change that occurred. Instead, the large-scale residual circulation changes are more associated with increased eddy energy (Table 2) and the Eliassen-Palm (EP) flux convergences that occur. When the EP forcing above the level of maximum streamfunction change is integrated and converted to a meridional mass flux equivalent, it approximates the actual change in residual circulation mass flux. The question then is

why the eddy energy in the middle atmosphere increased.

The change of annual-average EP fluxes with latitude in STRAT are presented in Fig. 5, along with the zonal wind changes. (It should be noted that because of the difficulty in generating completely accurate diagnostics for higher-order quantities such as EP fluxes and divergences in GCMs, these changes should be looked upon as being only approximate.) Increased upward wave energy fluxes occur in the troposphere at lower midlatitudes in both hemispheres ($\sim 30^\circ\text{N}$, 40°S). The energy then propagates upward and equatorward, leading to EP flux convergences at low to subtropical latitudes in the middle atmosphere. This is the primary cause for the acceleration of the residual circulation cells (Fig. 4a). The vertical energy propagation occurs primarily through regions of decrease in the tropospheric midlatitude west winds.

The explanation for the tropospheric changes is as follows. The warming due to the stratospheric aerosols in the lower stratosphere helps reduce the intensity of

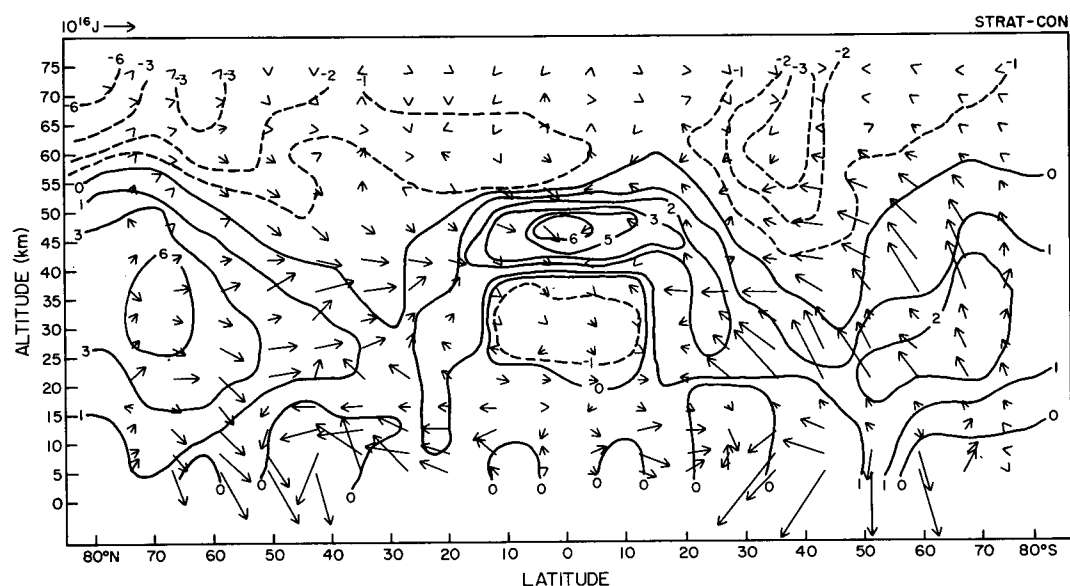


FIG. 5. Annual average change in EP flux (arrows) and zonal winds (contours). The EP fluxes have been reduced by a factor of 30 below 20 km, and by a factor of 5 from 20 to 35 km for presentation purposes. Negative zonal wind changes are dashed. (Notice that in this figure the Northern Hemisphere is on the left.)

the Hadley cell. The process through which this occurs involves the effect of increased vertical stability on the mean circulation cells in the troposphere. From a theoretical standpoint, the mean streamfunction intensity is inversely proportional to static stability [for example, see Rind and Rossow 1984, Eqs. (3) and (5)]. In STRAT, on the annual average, the increase in tropical tropospheric static stability is approximately 2%, while the decrease in the Hadley Cell is 1.4%, so the changes are the proper similar order of magnitude.

Along with the Hadley cell decrease is a decrease in subsidence at 27°N of 10%, an effect that is amplified by the model compared to the results for the Hadley cell as a whole, possibly because of a CISK-type feedback that maximizes its impact in regions of little rainfall. With reduced downward velocities in the subtropics, the model generates more rain there. This then is associated with a change in the subtropical to midlatitude precipitation gradient of 7.5%.

This additional heat-release gradient produces a more direct circulation, and, along with the increased static stability, helps reduce the Ferrel cell, on the order of 5% (note the more negative residual streamfunction at Northern Hemisphere midlatitudes in Fig. 4a). It also perturbs the energy flow. The Ferrel cell, with relatively cold air rising at higher latitudes and warmer air sinking at lower latitudes, is an indirect cell, driven by eddy kinetic energy. It is indicative of a transformation of zonal kinetic energy into zonal available potential energy. The more direct cell produced in association with the subtropical latent heat release reverses this energy flow: Now more zonal available potential energy goes to zonal kinetic energy, and then into eddy kinetic energy. Thus, the zonal kinetic energy is the direct source for the model's increase in standing eddy energy in this experiment. The outcome is that standing eddy kinetic energy increases by 9% in the Northern Hemisphere upper troposphere and zonal winds decrease at midlatitudes.

The reasons for the increased eddy energy in the middle atmosphere appear to differ in the two hemispheres. The eddy kinetic energy changes for the different levels and experiments are given in Table 2. Stratospheric increases occur for both hemispheres in both TRANS and STRAT, and are generally on the order of 5%, equivalent to two standard deviations. Tropospheric increases in eddy energy occur in the Northern Hemisphere in STRAT, especially in the standing eddies and in waves 1–4, of particular importance to increased stratospheric eddy energy. However, in the Southern Hemisphere standing wave energy and eddy energy in general is slightly reduced. In both hemispheres reduced west winds at middle latitudes allow for better energy propagation (Fig. 5). Apparently alterations in both tropospheric eddy energy and propagation conditions are responsible for the EP flux changes shown in Fig. 5. In addition, the possibility exists that the aerosol tropical heating, which increases the latitudinal temperature gradient in the lower

stratosphere, helps excite in situ eddy energy that then propagates vertically, an effect that could occur in both hemispheres.

The results shown in Fig. 5 help explain the dynamically induced temperature changes (Fig. 4b). The EP flux convergences in the stratosphere help generate the increased residual circulation responsible for the warming at upper-stratosphere polar latitudes, and cooling in the tropical middle-to-upper stratosphere. The EP flux divergence at polar latitudes in the upper troposphere and lower stratosphere is associated with increased west winds in those regions, and polar cooling. Reduction in EP fluxes at upper levels provides for reduced eddy energy near the model top in the mesosphere (Table 2). This results in a reduction in the divergence of vertical sensible heat flux that occurs at these levels (see the discussion in paper A), and relative warming. The effect is amplified by the presence of the model top, so must be considered quantitatively uncertain.

To summarize the results from this experiment, first for the troposphere and low- to midstratosphere: The introduction of stratospheric aerosols warms the lower stratosphere from the tropics through midlatitudes, cools the lower stratosphere at high latitudes, and produces some cooling in the troposphere during the first three years. The increased vertical stability weakens the Hadley cell, and increases subtropical precipitation; in response, the Ferrel cell weakens, and there is a relative transformation of zonal to eddy kinetic energy. The net effect is an increase in standing eddy energy and a decrease in midlatitude west winds, which leads to increased wave energy propagation toward midlatitudes in the troposphere, and subsequent propagation into the stratosphere. The relative EP flux divergence north of midlatitudes is associated with increased zonal winds, and polar cooling from the upper troposphere through the midstratosphere.

Additional eddy energy propagates into the middle atmosphere, although whether this is solely the result of the energy propagation from the troposphere is uncertain; warming of the tropics and cooling near the poles in the lower stratosphere increases zonal available potential energy and may be responsible for in situ energy generation in both hemispheres. The increased eddy energy helps drive an increased equator to pole residual circulation, an effect that is also aided by the direct aerosol warming. This produces cooling throughout the middle and upper stratosphere in the tropics, and warming in the upper stratosphere and mesosphere at polar latitudes, in both hemispheres.

b. TRANS

This experiment allowed the troposphere to respond to the increased volcanic aerosols for the first three years. The annual average temperature changes are presented in Fig. 1b. The middle atmosphere results are very similar to those in STRAT, while in the tro-

posphere there is somewhat greater cooling, especially in the Northern Hemisphere. However, in the Southern Hemisphere high latitudes are actually slightly warmer, as the interannual variability of sea surface temperatures is larger than the net radiative forcing induced in this experiment.

The explanations for the temperature changes are very similar to those discussed in STRAT, which validates their interpretation. This is important given that the changes are generally small, and of marginal significance. One difference that arises is due to the tropospheric high-latitude warming this experiment experienced in the Southern Hemisphere. Tropospheric eddy energy is reduced in this hemisphere more than was the case in STRAT (Table 2), and so the stratospheric eddy energy increase is less. The residual circulation increase is also reduced somewhat, as are the temperature changes associated with it: both the high-latitude warming and the tropical cooling near the stratopause are reduced by about 0.5°C. The Southern Hemisphere results are somewhat of an artifact of the 9-layer model's sea surface temperature variability, but they do serve to indicate the sensitivity of the system to tropospheric changes.

c. CLIM

In this experiment the sea surface temperatures have been given ample time to adjust, and thus have cooled substantially. The global average surface air temperature is now 4.7°C cooler. The latitudinal temperature change profile is shown in Fig. 6 for the annual average (Fig. 6a), December–February (Fig. 6b), and for June–August (Fig. 6c). Features that CLIM has in common with STRAT include:

- 1) warming in the tropical lower stratosphere due to additional shortwave and longwave absorption and
- 2) warming in the mesosphere near the model top, primarily a dynamic effect, as discussed for STRAT.

CLIM differs from STRAT in the following ways:

- 1) Tropospheric cooling is much more intense, as expected given the greater response of the sea surface temperatures.
- 2) Above the lower stratosphere the tropics has less consistent cooling, limited to the middle stratosphere immediately above the warmed regions.
- 3) The upper stratosphere in the extratropics cools, in general, in contrast to the warming experienced previously, and the Northern Hemisphere lower stratosphere undergoes much larger cooling.
- 4) There is now a substantial difference in temperature response in the middle atmosphere of the two hemispheres.

Outside of the lower tropical stratosphere, the stratospheric response in CLIM is markedly different from those of STRAT and TRANS. The shortwave stratospheric heating rate (Fig. 7a) increases in the tropical and Southern Hemisphere middle atmosphere

more so than in STRAT, because of a greater increase in tropospheric cloud cover, which acts to reflect radiation back to the stratosphere. In the GISS model, low-level cloud cover increases in cooler climates and decreases in warmer climates (Rind 1986), providing a positive feedback to the original climate forcing; in CLIM, low-level clouds increase by 7% relatively (from 36.5% to 39.1%). In the tropics high-level clouds increase as well (by close to 70% relatively), reducing shortwave absorption at those levels.

The tropical effect results in part from an increase in tropospheric tropical eddy energy (by a factor of two in the upper troposphere, and 10% overall). In the GISS model moist convection mixes momentum, which reduces wind gradients and thus eddy energy. In the colder climate of CLIM, penetrative moist convective mass flux is reduced (by 27% at 346 mb), and the eddy energy loss by this process is reduced (by 15% in the tropics). The increase in both low and high clouds leads to a total cloud cover change of 50% relatively (from 34% to 51%), raising the tropical planetary albedo by 15% relatively, and augmenting the tropical cooling substantially in comparison with the control run.

The greater cooling of the troposphere also implies reduced longwave energy losses (Fig. 7b), especially pronounced in regions of the tropical upper-tropospheric cooling, and this reduces longwave absorption from CO₂ and ozone in the stratosphere. Once again the thermal radiation cooling rate change is also affected by dynamical heating changes, of which it is practically a mirror image (Fig. 8b) (compare also Figs. 3b and 4b for STRAT).

The change in dynamical forcing also varies between the experiments, which accounts for much of the differing stratospheric temperature response. In the Northern Hemisphere, the residual circulation weakens (Fig. 8a), reducing the dynamical heating through most of the stratosphere (Fig. 8b). In the Southern Hemisphere the residual circulation generally increases, providing some additional dynamical heating in the polar region, especially in winter (Fig. 8b). Remember that in STRAT the residual circulation increased in both hemispheres (Fig. 4a).

This hemispheric differentiation is noticeable in the eddy energy change (Table 2); the Southern Hemisphere troposphere shows an increase in eddy energy, while the Northern Hemisphere has little change overall. This effect is related to the change in latitudinal temperature gradient: As is evident in Fig. 6, the greatest cooling in the low- and midtroposphere is found in the extratropics in the Southern Hemisphere due to the large expansion of sea ice. At similar levels in the Northern Hemisphere there is little overall increase in latitudinal temperature gradient, for the tropical cooling is similar to that in the extratropics. Thus, available potential energy increase is large in the Southern Hemisphere leading to increased eddy energy—effects that are missing in the Northern Hemisphere.

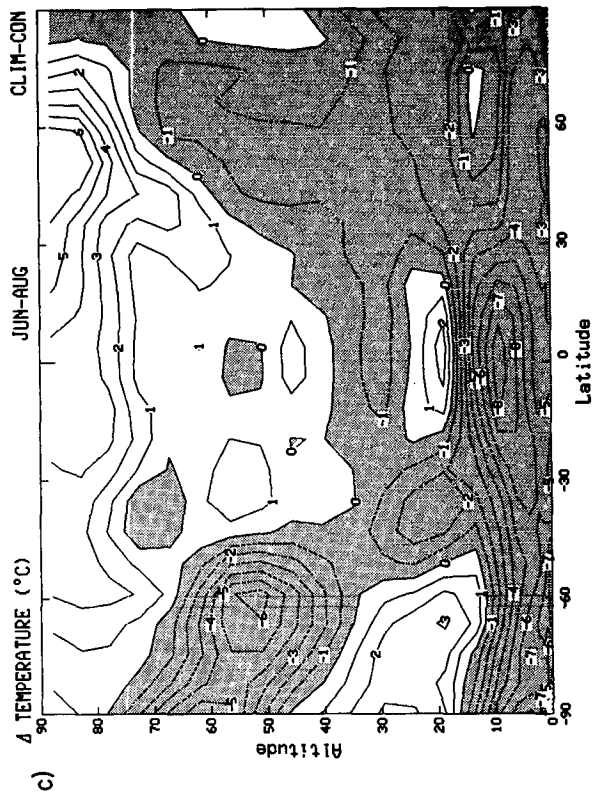
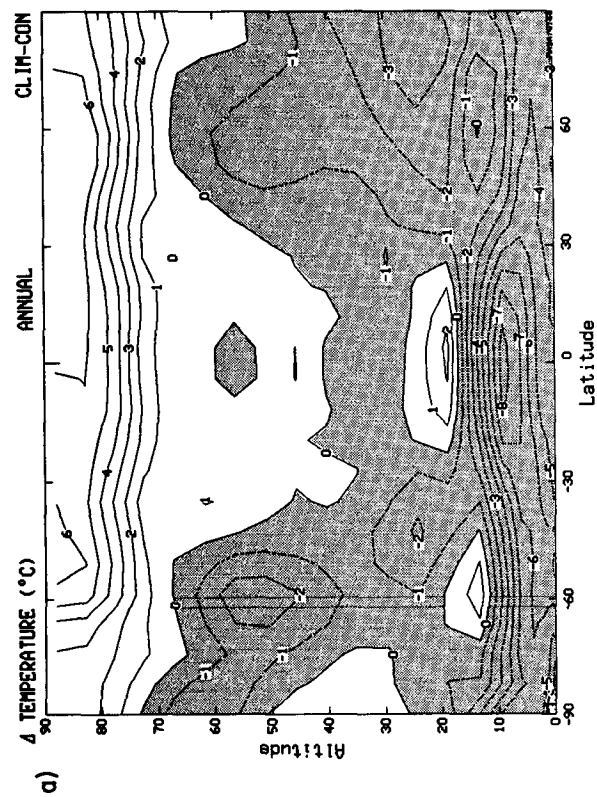
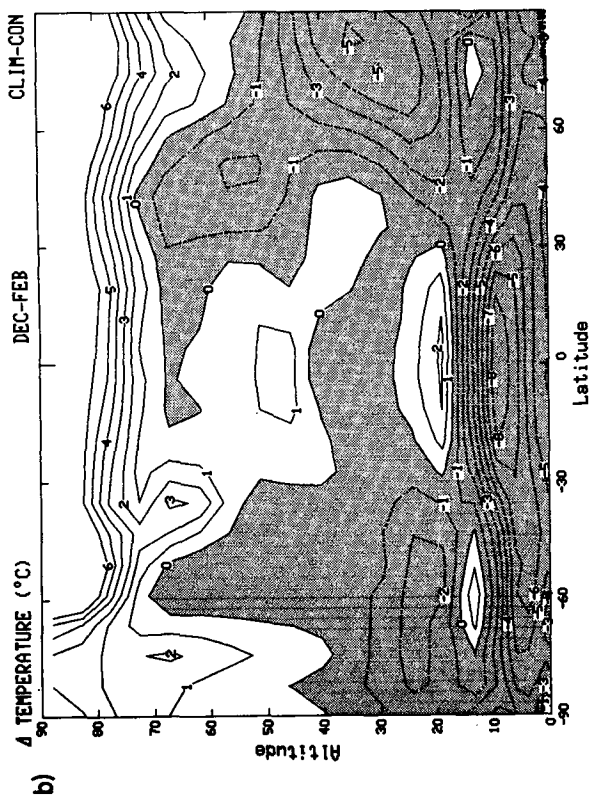


FIG. 6. Temperature change between CLIM and the current climate control run for (a) the annual average, (b) December-February, and (c) June-August.

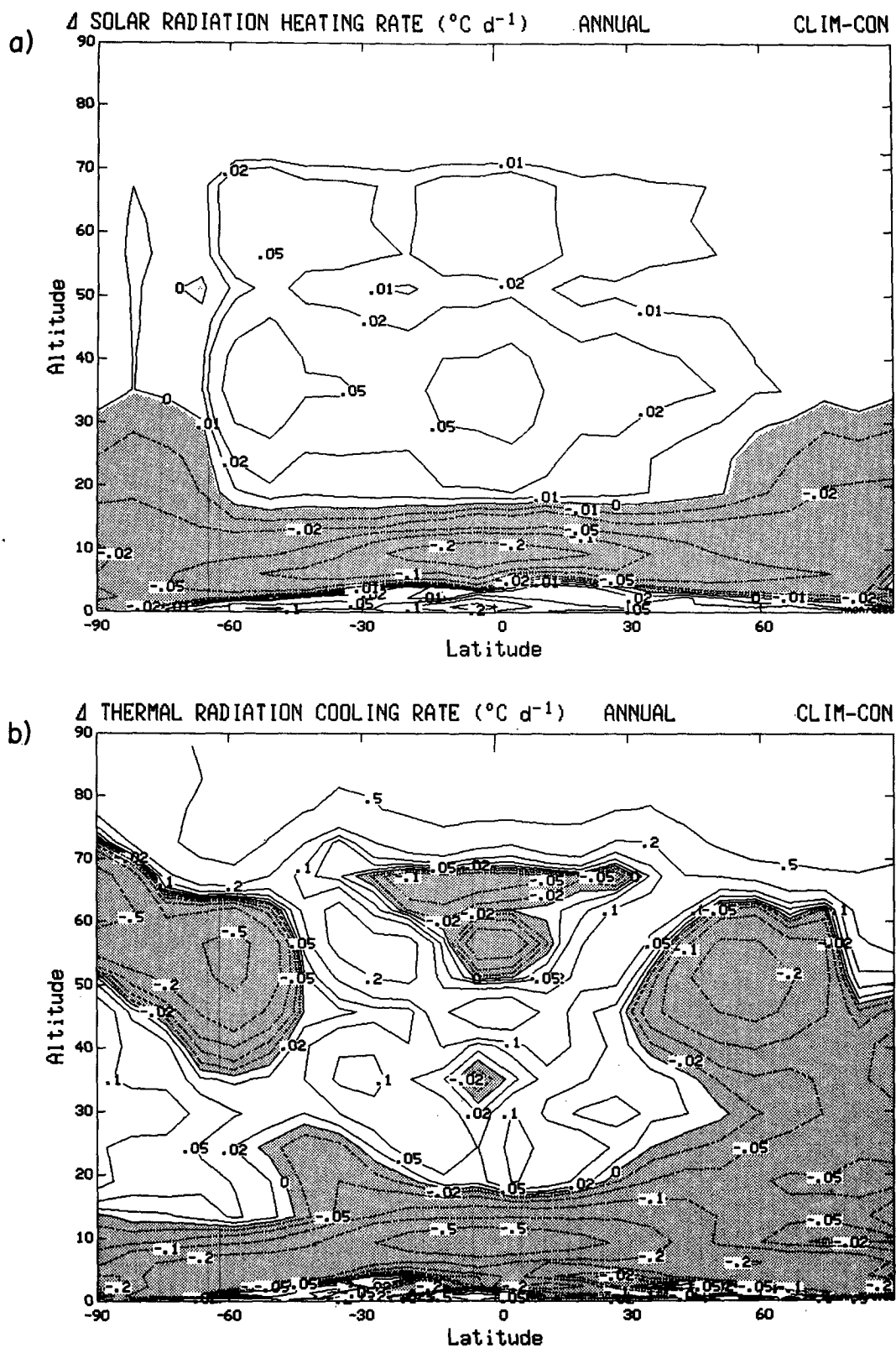


FIG. 7. As in Fig. 3 except for CLIM—control.

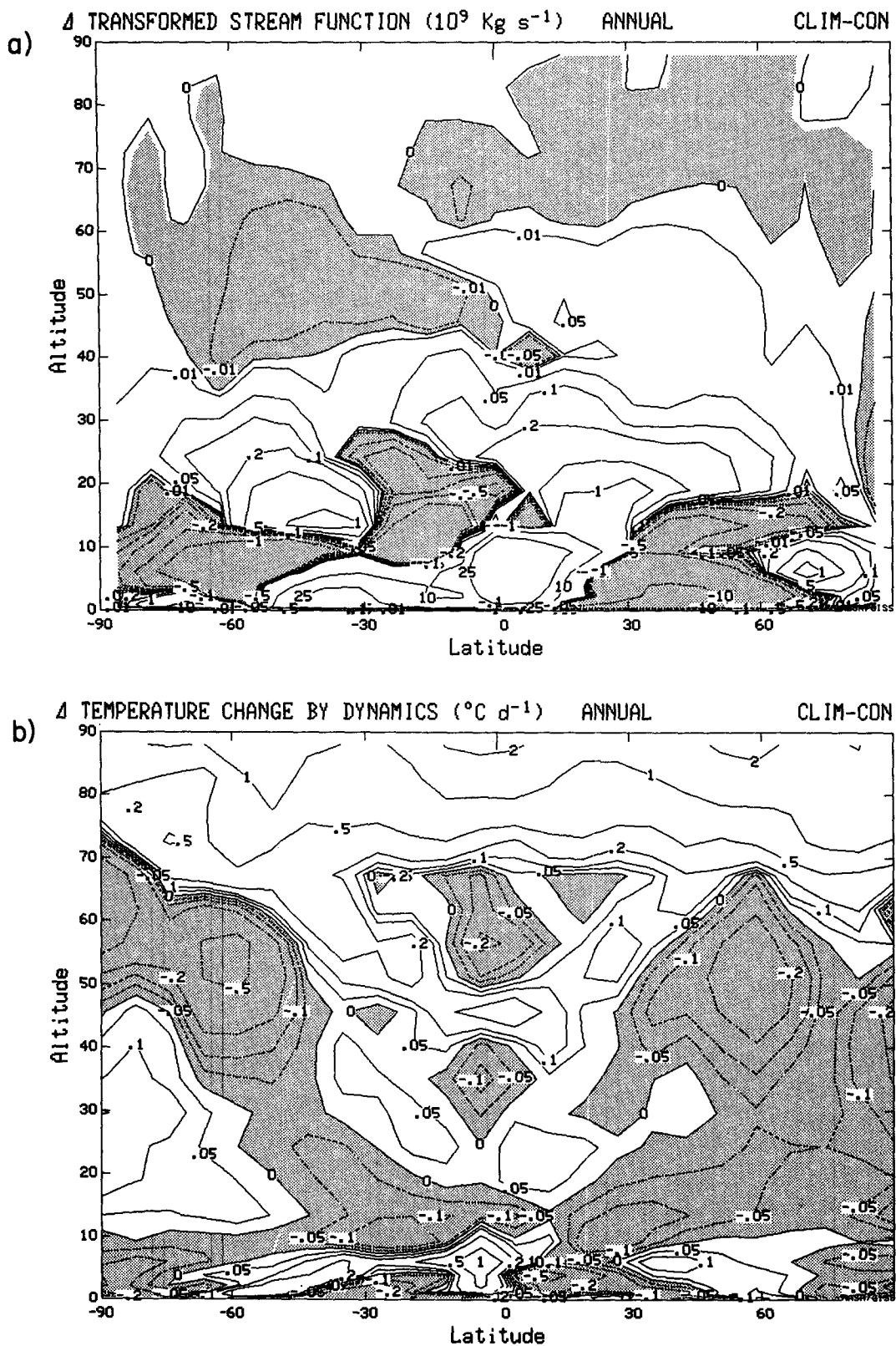


FIG. 8. As in Fig. 4 except for CLIM—control.

Eddy energy changes in the middle atmosphere are also greater in the Southern Hemisphere. Some additional vertical propagation of wave energy is possible in the Northern Hemisphere, despite a lack of tropospheric eddy energy increase, due to the weakening of the zonal west winds (Fig. 9). One effect of the tropospheric cooling is to reduce the upper-tropospheric latitudinal temperature gradient, by reducing tropical convection and heating. From the thermal wind relationship, this effect reduces the zonal winds and makes extratropical energy propagation easier. However, in general, this additional eddy energy does not propagate through the tropopause—most likely because of the decrease in the energy of wavenumbers 1–4 (by some 5%). In contrast, in the Southern Hemisphere, where planetary longwave energy increases, greater vertical EP fluxes propagate through the upper troposphere. This is especially true in the subtropics, where zonal winds decrease, consistent with the thermal wind relationship, due to the greater tropical cooling. Once again it is impossible to rule out a direct contribution from energy generated in the lower stratosphere, as available potential energy increases there. To the extent that this effect exists, it obviously does not dominate the results in the Northern Hemisphere.

The eddy energy change leads to some apparent differences in the appearance of stratospheric warmings. The major change is in the Southern Hemisphere, where two of the three winters had more obvious warming episodes than occurred in the control run. With the limited sampling available, the significance of this change is uncertain.

To summarize, with the extended duration of volcanic aerosol influence in the climate model, the sea surface temperatures were allowed to fully respond,

and the troposphere cools substantially. Less longwave energy is therefore radiated to and absorbed in the middle atmosphere, which contributes to its overall cooling. Slightly greater shortwave absorption occurs in the middle atmosphere due to an increase in tropospheric cloud cover, and thus additional reflected solar radiation. However, the main impact on the middle atmosphere comes from the distribution of the cooling with latitude in the midtroposphere: in the Northern Hemisphere, where the tropics cool more than high latitudes, eddy energy decreases, while in the Southern Hemisphere, where sea ice grows substantially, eddy energy increases. The eddy energy changes are replicated in their effect on the middle atmosphere with a decreased residual circulation in the Northern Hemisphere and cooling, and an increased extratropical residual circulation in the Southern Hemisphere and polar warming during winter.

4. Discussion

a. STRAT and TRANS

The results of the different experiments provide interesting examples of how potential climate perturbations, such as the input of volcanic aerosols, can affect the middle atmosphere in a model. The effects are a combination of direct stratospheric forcing and altered tropospheric forcing. The question to be addressed in this section is how relevant are these results to what occurs in the real world; that is, are the mechanisms for change that occur in the model an accurate reproduction of the mechanisms in the real atmosphere?

To assess the validity of the model results, we can compare the changes induced in the model in STRAT and TRANS with what has occurred after recent vol-

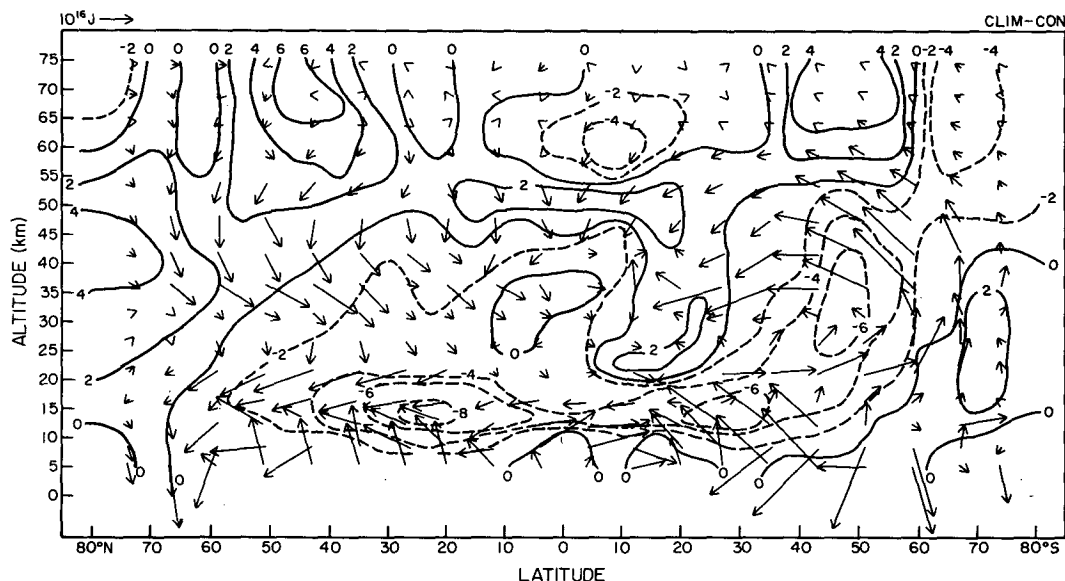


FIG. 9. As in Fig. 5 except for CLIM—control.

canoes. The model used an aerosol input with an optical depth of 0.15; this is approximately the value of the Mt. Agung aerosol (which erupted in 1963) by the beginning of 1964, and also approximately the value for the El Chichón aerosol (which erupted in 1982) by the beginning of 1983 (see the discussion in Hansen et al. 1988, appendix B). The properties for the aerosols are approximately those observed for these two volcanoes. The aerosols are put in uniformly as a function of latitude, which is certainly not a good assumption for time periods close to the volcanic eruption date, but becomes somewhat better within the first year (e.g., Dutton and DeLuisi 1983). Thus, the comparison cannot be exact, but should be qualitatively similar to "real world" effects.

Another question of concern: What are the real world effects? As emphasized by Quiroz (1983), stratospheric changes that followed the volcanic eruption must be separated from changes induced by other mechanisms, for example, the quasi-biennial oscillation in the tropical lower stratosphere. The same caveat applies with even greater validity in the troposphere, as interannual changes could obscure the volcanic aerosol signal. The following comparisons will obviously be limited by our lack of knowledge of what the volcanic signal really was.

For comparison purposes, substantial data are available for regions up to approximately 10 mb in both 1964 and 1983. However, in the troposphere, the 1982–83 time period also featured a very strong El Niño, which limits its usefulness for direct volcanic influence. At higher levels, global data from satellite analysis is restricted to the latter time period, although rocketsondes are available in the western hemisphere.

We begin with the lower stratosphere. As estimated by Quiroz (1983), among others, the El Chichón aerosols were responsible for a warming of 1°–3°C between the equator and 35°N. This assessment is in good agreement with the results in TRANS and STRAT (Fig. 1). Labitzke and Naujokat (1983) have shown that similar temperature changes can be ascribed to the Mt. Agung volcano [and Pinatubo (Labitzke and McCormick 1992)]. The warming is a result of both solar and thermal effects (Fig. 3). The solar radiation absorption occurs in the near infrared, and the thermal absorption is primarily a result of the larger (0.5 μm) particles included in the prescription.

The lower stratosphere cooling at higher latitudes is also in agreement with observations (van Loon and Labitzke 1987; Labitzke and van Loon 1989). It is produced, in part, radiatively by a decrease in solar radiation absorption and an increase in thermal radiation cooling (Fig. 3). Decreased solar radiation absorption at higher latitudes is a result of the zenith angle effect on the albedo of the small particles used in this experiment: With increased zenith angle the albedo rises rapidly, and scattering reduces the energy available for absorption by gases and aerosols more

than the additional absorption provided by the additional aerosols. This is why the solar radiation effect switches from warming to cooling in the lower stratosphere with an increase in latitude (Figs. 3a, 7a); note that aerosol-induced cooling at high latitudes may lead to an increase in polar stratospheric cloud formation. The scattered radiation is absorbed somewhat at higher levels, and thus polar regions of the upper stratosphere have a slight increase in shortwave absorption.

The high-latitude thermal radiation cooling is a result of the presence of aerosols above a cold surface. As discussed by Pollack and McKay (1985), volcanic particles enhance both the absorption of thermal radiation from other layers of the atmosphere and the emission of thermal radiation from the layers where they are located. When the contrast between the radiating layer (lower stratosphere) and the surface temperature is large, the particles warm, whereas at high latitudes, with little temperature contrast, they cool.

The importance of solar radiation absorption on producing the temperature changes in the lower stratosphere is in some disagreement with the analysis of Pollack and McKay (1985), as well as Hansen et al. (1978), which emphasized the thermal absorption contribution. The relative importance of these two factors is strongly dependent on the particle size and its distribution. The distribution used by Hansen et al. (1978) tended to produce a larger effective particle size, and thus a stronger thermal effect. To the extent that the distribution used here was indicative of the actual size distributions for Mt. Agung and El Chichón aerosols, this result should be more applicable.

The cooling at high latitudes in the lower stratosphere also has a dynamic component (Fig. 4b). This raises the question of whether the dynamical changes produced in the model occurred in the real atmosphere. In particular, the results shown in Fig. 5 indicate a relative EP flux away from high latitudes. The polar low-to-middle stratosphere experienced dynamically stable Northern Hemisphere winters following both of the major volcanoes, in contrast to what would have been expected from the QBO/solar cycle relationships (van Loon and Labitzke 1987; Labitzke and van Loon 1989). The model and observations are thus consistent, although we cannot be sure that the real world change was associated with the volcanic forcing. To explore this question, we need to relate the reasons for the model result to assessments of what happened in the real world.

In the model, the altered EP fluxes were part of a general reorganization of tropospheric energy flow, which featured reduced Hadley and Ferrel cells, reduced midlatitude zonal winds, and increased midlatitude standing wave energy (Fig. 5; Table 2). We concentrate on the winter of 1964 (Oort 1983), which is free of the El Niño influence that occurred in 1983. Shown in Fig. 10 are the observed changes for January 1964 (from Oort 1983, compared with the averages

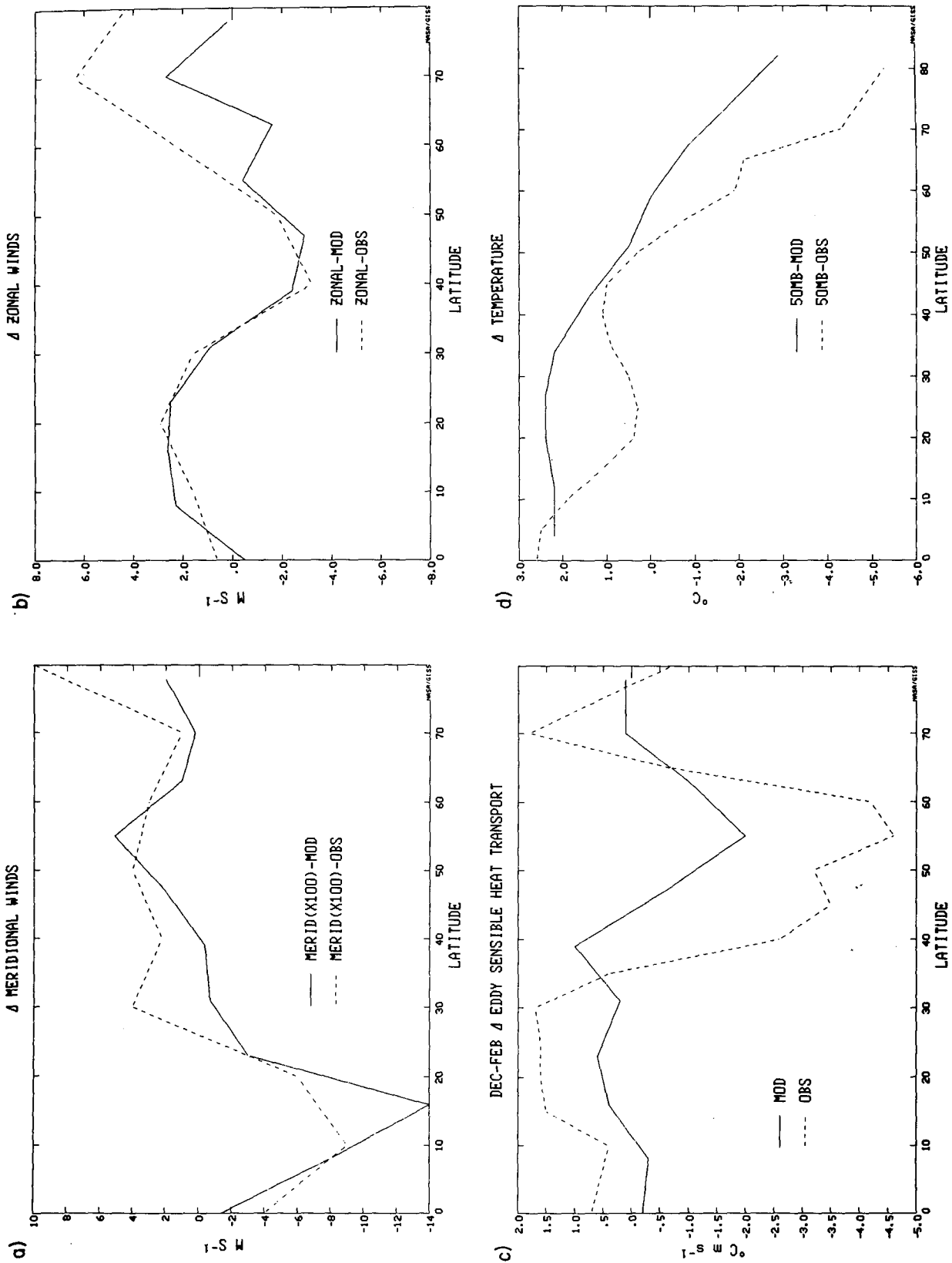


FIG. 10. Comparison of observed changes in January (1964) with those for December-February in STRAT for (a) 200-mb meridional wind (multiplied by 100); (b) 200-mb zonal wind; (c) 200-mb eddy transport of sensible heat; (d) 50-mb temperatures. Observations are from Oort (1983).

for 1963–73), and the modeled changes for December–February (3-year average) in STRAT. The observed circulation for January featured amplified ridges and troughs in their normal position, and this was true for December 1963 and February 1964 as well (with effects that were, if anything, even larger than those in January: Stark 1964; Andrews 1964; O'Connor 1964).

The Hadley and Ferrel cells decreased in both model and observations, as indicated by the decreased northward flow at 200 mb in the tropics, and the increased northward flow at 200 mb in midlatitudes (Fig. 10a). Zonal winds weaken at the same location in both model and observations (Fig. 10b); note that this is contrary to what would be expected from the Coriolis turning of the increased meridional wind at that latitude, and must be the result of eddy processes.

Standing eddy energy increased at upper midlatitudes in both model and observations, although the observed change was somewhat greater, averaging some 40% north of 40°N in Oort's data, compared with the model increase of 10%–25%. However, in both datasets there were compensating decreases in transient eddy energy, so the eddy transport of sensible heat in the upper troposphere increases only in the subtropics (Fig. 10c). As this term is the dominant contributor to the vertical EP flux, it implies that the observed wave energy propagation into the stratosphere was augmented primarily at subtropical and lower midlatitudes, as occurred in the model (Fig. 5). The relative convergence visible in Fig. 10c from 35°–55°N is true of the vertical derivative of eddy sensible heat transport as well, and implies relative EP flux convergence there in both the model and observations, helping to decelerate the zonal winds at these latitudes (Fig. 10b). Finally, the temperature changes as a function of latitude are similar, with cooling in the polar upper troposphere/lower stratosphere, and warming at low latitudes (Fig. 10d). All in all, the model simulation is in quite close agreement with the observations for the winter following the Mt. Agung eruption, with similar dynamic processes.

Was the observed response a direct result of the Mt. Agung aerosol? The changes observed during January 1964 were relatively large compared to those in other winters; for example, the tropical warming in the lower stratosphere was greater than that in any other January from 1958–73, while the cooling in the polar upper troposphere/lower stratosphere and the midlatitude zonal wind decreases were exceeded only once. Nevertheless, with only one unambiguous example of the effect of a large volcano on the troposphere, it is impossible to verify cause and effect. At the very least, the similarity between the modeled and observed response is suggestive of a causal connection.

Comparisons of the results with the winter following El Chichón are made more difficult because of the overwhelming influence of the El Niño event of 1982–83. There has been much speculation about whether

this El Niño was influenced by the volcano that erupted just prior to it (e.g., Handler 1984). The results from STRAT and TRANS suggest a possible connection, as a weakened Hadley cell would make El Niño events more likely, since it is the trade winds associated with the Hadley cell that help confine warm water to the western Pacific. Whether the small magnitude of the changes produced in this experiment would be sufficient to trigger the event depends on the (relatively unknown) sensitivity of the system. The magnitude of the Hadley cell changes in the model also vary with season: during December through February, the subtropical portion of the Hadley cell decreases in STRAT by 5%, and this is the season in which El Niños normally maximize.

What about conditions at higher levels? The model simulation produces cooling in the tropical middle and upper stratosphere, and warming in the extratropical upper stratosphere and mesosphere. During the winter of 1963/64 only observations from the Meteorological Rocket Network were available. Apparently at the upper levels (0.4 and 2 mb), the winter was dominated by a “quite active anticyclone” . . . , with periods of intense height and temperature increases” over Alaska and Canada (NMC 1967). While these results are again suggestive, no comparisons with climatology or general hemispheric coverage are available.

Parker and Brownscombe (1983) show results comparing tropical and global temperatures in 1980, 1981, and 1982 produced by the NOAA 6 Stratospheric Sounding Unit and Microwave Sounding Unit radiance channels. Following the eruption of El Chichón, the warming in the tropical lower stratosphere is accompanied by temperature changes in the upper stratosphere (2 mb) consistent with the model results: cooling in the tropical upper stratosphere and warming in the extratropics, by up to 2°C in both regions. There is no proof as such that the results came about due to an altered residual circulation, but the latitudinal and altitudinal characteristics of the changes are consistent with such an effect, and Dunkerton and Delisi (1991) recently concluded that the upper stratosphere cooling was not a radiative response.

To the extent, then, that verification is possible, the model results are consistent with happenings after the major volcanoes. The model results are physically plausible and understandable; however, it will take additional large volcanic eruptions (e.g., Pinatubo) before we can have confidence that the model's troposphere and middle atmosphere are responding in a manner similar to that of the real atmosphere.

b. CLIM

The results from CLIM are potentially applicable to climate epochs in which significant amounts of volcanic dust remained in the atmosphere for extended periods of time. Porter (1986) suggested that increased vol-

canicity could have been responsible for the cooling during the Little Ice Age, as acidity records in the Greenland ice core, indicative of volcanicity, match well with records of mountain glacier advances in the Northern Hemisphere. The ice line descent of about 160 m is one-fifth that which occurred during the last ice age (e.g., Rind and Peteet 1985). Assuming the global temperature change was similarly related, and that the ice age cooling was on the order of 5°C , this would imply a global cooling of $\sim 1^{\circ}\text{C}$ for the Little Ice Age.

CLIM used an aerosol optical thickness equivalent to a 2% reduction in solar constant to produce a 5°C global cooling. As values within this range are linear, we can estimate that $\sim 0.4\%$ solar constant reduction would have been needed for the Little Ice Age, with the GISS climate model sensitivity. However, the GCMAM was not in radiative equilibrium with the sea-surface temperature input from the 9-level climate model. The GISS climate model has a sensitivity of $\sim 1^{\circ}\text{C}/\text{W m}^{-2}$, and the GCMAM with exactly the same physics should have approximately the same sensitivity. CLIM is out of balance by $\sim 1 \text{ W m}^{-2}$; if its sea surface temperatures had been allowed to adjust it would have cooled about 1°C less, implying $\sim 0.5\%$ solar constant reduction for the Little Ice Age. In either case, the optical thickness used in CLIM is significantly more than that which likely occurred in the Little Ice Age, so the results shown for this experiment will represent an exaggeration of what might have occurred during the Little Ice Age if volcanic aerosols were the cause.

With that perspective, we can review what the model suggests would be the likely changes for such a time period. The middle-atmosphere responses in the two hemispheres are completely different, a result of the differing reactions in their respective tropospheres. The Northern Hemisphere troposphere features reduced eddy energy, especially in the planetary long waves, while the Southern Hemisphere troposphere has increased eddy energy. Offhand, the reduced eddy energy in the Northern Hemisphere is a surprise; the canonical view of colder climates is that cooling should maximize at high latitudes, increasing the latitudinal temperature gradient and baroclinic generation of eddies. There is some increased baroclinic generation, but the effect is not dominant because the results show very little high-latitude temperature change amplification in this hemisphere (Fig. 6). The reasons behind this result are discussed below, and in Pollack et al. (1991).

The volcanic aerosols scatter sunlight back to space, and directly produce about 30% of the cooling of the troposphere. As incident sunlight maximizes at low latitudes, the aerosol-induced reduction is about twice as large there compared with 60° latitude. This effect is amplified by the increased cloud cover in the tropics noted previously. Furthermore, it is recognized that the high stability of the winter polar atmosphere restricts temperature changes to low levels, in comparison

with the tropical situation in which convection redistributes changes to all altitudes. However, when the atmosphere cools, penetrative convection becomes less frequent, so the efficiency of redistribution in the tropics is reduced. The result is that the latitudinal variation of the tropospheric vertically integrated temperature change is very similar to that of the surface temperature change in the Northern Hemisphere.

Without the strong increase in cooling with increasing latitude, baroclinic eddy generation is not overly enhanced. What about the mechanism that produced additional eddy energy in TRANS and STRAT, the conversion of zonal kinetic energy to eddy energy, due to the altered Hadley and Ferrel circulations? A reduction in the Hadley cell also occurs in CLIM, associated with the increased tropospheric stability, as well as reduced evaporation/precipitation at low latitudes resulting from the cooler sea surface temperatures. This would imply increased rainfall in the subtropics, as in the previous experiments; however, with the cooler sea surface temperatures of CLIM, evaporation is severely restricted in the subtropics, which then leads to a reduction in subtropical precipitation. Thus, the Ferrel cell does not show as strong a decrease, and eddy generation associated with transformation from zonal kinetic energy is smaller than in STRAT.

Nevertheless, despite these effects, tropospheric eddy energy in the Northern Hemisphere would not have shown a decrease were it not for one other process. As noted in section 3b, the colder climate led to reduced penetrative convection and more eddy kinetic energy in the tropics. However, the GISS convection scheme tends to overstabilize the atmosphere. When penetrative convection decreases, low-level convection increases (see the discussion in Rind 1988). Increased convective mixing of momentum at lower levels in the extratropics then results in reduced eddy energy. Therefore, the Northern Hemisphere response of decreased tropospheric eddy energy in the planetary long waves depends upon the latitudinal distribution of temperature change produced in the GCM, as well as details of its convection scheme. With reduced Northern Hemisphere tropospheric planetary longwave energy, there is a reduced vertical flux of energy into the lower stratosphere, reduced EP flux convergences in the stratosphere, reduced residual circulation, and widespread cooling.

How about in the Southern Hemisphere? Here the model does produce a significant amplification in high-latitude cooling, associated with the increase in sea ice at polar latitudes. Thus, baroclinic energy generation increases substantially, as does tropospheric eddy energy. There is an increased vertical flux of energy into the lower stratosphere, increased EP flux convergences in the stratosphere, an increased residual circulation, and some warming. The validity of the large sea ice response is open to question: the GCM lacks a dynamic ocean/sea ice model, and it is uncertain whether sea ice could extend as far equatorward as implied by the

model. Nevertheless, during the last ice age the Southern Hemisphere sea ice response was thought to have been a factor of 10 larger than in the Northern Hemisphere (CLIMAP 1981), and if this is true for colder climates in general, it could imply a hemispheric asymmetry in tropospheric and middle-atmosphere reaction.

It is interesting to note that the temperature changes generated in the middle atmosphere in CLIM are not much greater than those in STRAT and TRANS, at least on the annual average (compare Figs. 1 and 6), despite the fact that CLIM has much greater tropospheric cooling. Apparently, the myriad of feedbacks that arise limit a straightforward translation of tropospheric magnitudes of change to changes in the middle atmosphere.

5. Conclusions

The influence of volcanic aerosols on the middle atmosphere can be divided into three categories: the direct effect on the stratosphere itself, the direct effect on the troposphere, and the tropospheric changes that arise from the direct effect on the stratosphere and then feed back on the middle atmosphere. The direct effect on the stratosphere, namely, warming of the tropical lower stratosphere and cooling of the polar lower stratosphere, occurred in all the experiments. The tropospheric changes depended upon the length of time the aerosols were allowed to act.

Within the first several years, a period similar to that of the influence of major volcanoes in this century, the warming of the lower stratosphere led to an increase in tropical static stability, a reduction in Hadley cell and Ferrel cell intensities, a reduction in midlatitude westerlies, and an increase in wave energy flux into the stratosphere at subtropical and lower midlatitudes. The additional wave energy flux convergences, along with the direct lower-stratospheric radiative heating of the aerosols, intensified the residual circulation in both hemispheres, leading to some high-latitude warming and low-latitude cooling in the upper stratosphere and lower mesosphere. The dynamical changes are generally on the order of 10%. To the extent possible, we have shown that the real world atmospheric response following Mt. Agung and El Chichón had many similarities to the results generated in these experiments.

When the aerosols were allowed to remain in the atmosphere sufficiently long to cool the troposphere to a new equilibrium level (some 50 years), a hemispheric asymmetry in middle-atmosphere response became apparent. In the Northern Hemisphere there was a reduction in tropospheric planetary long-wave energy, which translated into reduced wave energy flux into the stratosphere, a diminished residual circulation, and widespread cooling. In contrast, in the Southern Hemisphere, the large sea ice response to the global cooling substantially increased the latitudinal temperature gradient, leading to increased eddy energy, in-

creased wave energy flux into the stratosphere, an amplified residual circulation, and some high-latitude warming.

Both experiments emphasize that the middle-atmosphere response to climate change depends on both the direct and indirect (i.e., tropospheric) effects. Similarly, the tropospheric changes are not simply the products of the direct climate perturbation; they depend as well on what happens to the stratosphere. In Part I of these studies (RSBP), stratospheric cooling in conjunction with tropospheric warming decreased the static stability, allowing for greater planetary long-wave energy generation in the troposphere, which then propagated into and influenced the middle atmosphere. In these experiments the increased static stability in the tropics altered the Hadley circulation, which affected tropospheric eddy energy, its propagation into the stratosphere, and the subsequent middle-atmosphere effects. These examples of the coupled systems emphasize the need to include both the troposphere and middle atmosphere in studying the effects of climate change.

As noted in the introduction, there has been speculation that the Little Ice Age may have resulted in part from increased volcanic activity, and this is true of other cold epochs during the last 1000 years (Porter 1986). Alternate explanations concern the possibility for solar constant change associated with the Maunder Minimum sunspot decrease (e.g., Eddy 1976). We may expect that reduced solar insolation would have a different impact on the middle atmosphere, and thus perhaps on the troposphere, than volcanic aerosols, for reduced solar insolation should cool the stratosphere. Interpretation of the paleorecord may be aided by comparing such experiments and looking for their varying influences, either on the potential for altered ozone distributions or direct tropospheric effects as mediated by the middle atmosphere. The effect of reduced solar isolation on the middle atmosphere will be the focus of a subsequent part of this series.

Acknowledgments. We thank James Pollack and James Hansen for their impetus in formulating and running the volcanic aerosol experiment with the 9-level climate model, and subsequent discussion of its results. Andy Lacis provided valuable insight into the radiative effects of the volcanic aerosols. Patrick Lonergan helped with computer processing of the results, and Lilly Del Valle helped in preparation of the figures. This work was supported by the NASA Upper Atmosphere Program Office.

REFERENCES

- Andrews, J. F., 1964: The weather and circulation of January, 1964. *Mon. Wea. Rev.*, **93**, 189–194.
- CLIMAP Project Members, 1981: *Seasonal Reconstruction of the Earth's Surface at the Last Glacial Maximum*, Geol. Soc. Amer. Map and Chart Series MC-36.
- Dunkerton, T. J., and D. P. Delisi, 1991: Anomalous temperature

- and zonal wind in the tropical upper stratosphere, 1982/1983. *J. Geophys. Res.*, **96**, 22 631–22 641.
- Dutton, E., and J. DeLuise, 1983: Spectral extinction of direct solar radiation by the El Chichón cloud during December 1982. *Geophys. Res. Lett.*, **10**, 1013–1016.
- Eddy, J. A., 1976: The Maunder Minimum. *Science*, **192**, 1189–1202.
- Fujita, T., 1985: The abnormal temperature rises in the lower stratosphere after the 1982 eruptions of the volcano El Chichón, Mexico. *Papers in Meteor. and Geophys.*, **36**, 47–60.
- Handler, P., 1984: Possible association of stratospheric aerosols and El Niño type events. *Geophys. Res. Lett.*, **11**, 1121–1124.
- Hansen, J. E., W.-C. Wang, and A. Lacis, 1978: Mount Agung eruption provides test of a global climatic perturbation. *Science*, **199**, 1065–1068.
- , G. Russell, D. Rind, P. Stone, A. Lacis, S. Lebedeff, R. Ruedy, and L. Travis, 1983: Efficient three-dimensional global models for climate studies: models I and II. *Mon. Wea. Rev.*, **111**, 609–662.
- , —, A. Lacis, I. Fung, D. Rind, and P. Stone, 1985: Climate response times: dependence on climate sensitivity and ocean mixing. *Science*, **229**, 857–859.
- , I. Fung, A. Lacis, D. Rind, S. Lebedeff, R. Ruedy, and G. Russell, 1988: Global climate changes as forecast by Goddard Institute for Space Studies three-dimensional model. *J. Geophys. Res.*, **93**, 9341–9364.
- Hofmann, D. J., and J. M. Rosen, 1983: Stratospheric sulfuric acid fraction and mass estimate for the 1982 volcanic eruption of El Chichón. *Geophys. Res. Lett.*, **10**, 313–316.
- Labitzke, K., and B. Naujokat, 1983: On the variability and on trends of the temperature in the middle stratosphere. *Contrib. Atmos. Phys.*, **56**, 495–507.
- , and H. van Loon, 1989: The Southern Oscillation. Part IX: The influence of volcanic eruptions on the Southern Oscillation in the stratosphere. *J. Climatol.*, **10**, 1223–1226.
- , and M. P. McCormick, 1992: Stratospheric temperature increases due to Pinatubo aerosols. *Geophys. Res. Lett.*, **19**, in press.
- , B. Naujokat, and M. P. McCormick, 1983: Temperature effects on the stratosphere of the April 4, 1982 eruption of El Chichón, Mexico. *Geophys. Res. Lett.*, **10**, 24–26.
- National Meteorological Center, Upper Air Branch, 1967: Weekly synoptic analyses, 5, 2, and 0.4 mb surfaces for 1964. ESSA Tech. Rep. WB-2, 176 pp. [Available from NTIS, Springfield, Va., M(055)U5885te.]
- Newell, R. E., 1970: Stratospheric temperature change from the Mount Agung volcanic eruption. *J. Atmos. Sci.*, **27**, 977–978.
- O'Connor, J. F., 1964: The weather and circulation of February, 1964. *Mon. Wea. Rev.*, **93**, 255–261.
- Oberbeck, V. R., E. F. Danielsen, K. G. Snetsinger, and G. V. Ferry, 1983: Effect of the eruption of El Chichón on stratospheric aerosol size and composition. *Geophys. Res. Lett.*, **10**, 1021–1024.
- Oort, A., 1983: *Global Atmospheric Circulation Statistics*, NOAA Prof. Paper 14, U.S. Dept. of Commerce, 180 pp.
- Palmer, K. F., and D. Williams, 1975: Optical constants of sulfuric acid: application to the clouds of Venus? *J. Opt. Soc. Amer.*, **14**, 208–219.
- Parker, D. E., and J. K. L. Brownscombe, 1983: Stratospheric warming following the El Chichón volcanic eruption. *Nature*, **301**, 406–408.
- Pollack, J. B., and T. P. Ackerman, 1983: Possible effects of the El Chichón volcanic cloud on the radiation budget of the Northern tropics. *Geophys. Res. Lett.*, **10**, 1057–1060.
- , and C. P. McKay, 1985: The impact of polar stratospheric clouds on the heating rates of the winter polar stratosphere. *J. Atmos. Sci.*, **42**, 245–262.
- , D. Rind, A. Lacis, and J. Hansen, 1991: GCM simulations of volcanic aerosol forcing. I: Climate changes induced by steady state perturbations. *J. Geophys. Res.*, submitted.
- Porter, S. C., 1986: Pattern and forcing of Northern Hemisphere glacier variations during the last millennium. *Quart. Res.*, **26**, 27–48.
- Quiroz, R. S., 1983: The isolation of stratospheric temperature change due to the El Chichón volcanic eruption from nonvolcanic signals. *J. Geophys. Res.*, **88**, 6773–6780.
- Rind, D., 1986: The dynamics of warm and cold climates. *J. Atmos. Sci.*, **43**, 3–24.
- , 1988: Dependence of warm and cold climate depiction on climate model resolution. *J. Climate*, **1**, 965–997.
- , and W. Rossow, 1984: The effects of physical processes on the Hadley circulation. *J. Atmos. Sci.*, **41**, 479–507.
- , and D. Peteet, 1985: Terrestrial conditions at the Last Glacial Maximum and CLIMAP sea-surface temperature estimates: are they consistent? *Quat. Res.*, **24**, 1–22.
- , R. Suozzo, N. K. Balachandran, A. Lacis, and G. Russell, 1988a: The GISS global climate/middle atmosphere model. Part I: model structure and climatology. *J. Atmos. Sci.*, **45**, 329–370. (Part I)
- , —, and —, 1988b: The GISS global climate/middle atmosphere model. Part II: Model variability due to interactions between planetary waves, the mean circulation, and gravity wave drag. *J. Atmos. Sci.*, **45**, 371–386. (Part II)
- , —, —, and M. J. Prather, 1990: Climate change and the middle atmosphere. Part I: The doubled CO₂ climate. *J. Atmos. Sci.*, **47**, 475–494. (RSBM III)
- Stark, L. P., 1964: The weather and circulation of December 1963. *Mon. Wea. Rev.*, **93**, 139–146.
- van Loon, H., and K. Labitzke, 1987: The Southern Oscillation. Part V: The anomalies in the lower stratosphere of the Northern Hemisphere in winter and a comparison with the Quasi-biennial Oscillation. *Mon. Wea. Rev.*, **115**, 357–369.
- Wendler, G., and Y. Kodama, 1986: Some remarks on the stratospheric temperature for Fairbanks, Alaska after the El Chichón eruption. *Atmos.–Ocean*, **24**, 346–352.